Hindawi Publishing Corporation
Journal of Spectroscopy
Volume 2013, Article ID 321483, 9 pages
http://dx.doi.org/10.1155/2013/321483

Research Article

An Investigation of Nanocrystalline and Electrochemically Grown Cu_2ZnSnS_4 Thin Film Using Redox Couples of Different Band Offset

Prashant K. Sarswat,[1] Michael L. Free,[1] and Gagan Kumar[2]

[1] *Department of Metallurgical engineering, University of UT, Salt Lake City, Utah 84112, USA*
[2] *Institute for Research in Electronics and Applied Physics, University of Maryland, College Park, MD 20742, USA*

Correspondence should be addressed to Prashant K. Sarswat; saraswatp@gmail.com

Received 31 May 2013; Accepted 12 August 2013

Academic Editor: Yogendra Mishra

Alternative electrolytes were examined to evaluate photoelectrochemical response of Cu_2ZnSnS_4 films at different biasing potential. Selections of the electrolytes were made on the basis of relative Fermi level position and standard reduction potential. Our search was focused on some cost-effective electrolytes, which can produce good photocurrent during illumination. Thin films were grown on FTO substrate using ink of nanocrystalline Cu_2ZnSnS_4 particles as well as electrodeposition-elevated temperature sulfurization approach. Our investigations suggest that photoelectrochemical response is mostly due to conduction band-mediated process. Surface topography and phase purity were investigated after each electrochemical test, in order to evaluate film quality and reactivity of electrolytes. Raman examination of film and nanocrystals was conducted for comparison. The difference in photocurrent response was explained due to various parameters such as change in charge transfer rate constant, presence of dangling bond, difference in concentration of adsorbed species in electrode.

1. Introduction

In the last two decades, there has been significant interest in developing copper zinc tin sulfide, Cu_2ZnSnS_4 (CZTS) based solar cell devices. CZTS offers favorable optical and electronic properties suitable for solar cell applications. A tremendous improvement has been reported in the power conversion efficiency of CZTS device in the last few years [1]. Recently, 11.1% efficiency of photovoltaic device with standard configuration (glass/Mo/CZTSSe/CdS/ZnO/ITO/Ni-Al) reported by IBM indeed proves that CZTS will be a leading candidate for thin film environmentally friendly solar cell [2]. One of the great advantages of this material is utilization of abundant and cost effective constituent elements. Despite the fact of improvement in efficiency, many other shortcomings are also needed to be overcome such as low fill factor, reduced short circuit current, and high recombination due to secondary phases. In all cases, it is essential to examine device performance prior to fabrication of complete photovoltaic cell. In most of the time photovoltaic properties of CZTS absorber were examined using a "semiconductor-electrolyte interface" as a testing analog [3]. This facilitates easy formation of Schottky barriers using heterojunctions [3]. A nondestructive way of photovoltaic property evaluation is an additional benefit. It can be seen that in many cases Eu^{3+}/Eu^{2+} was utilized as a redox couple because of various associated advantages [3–5]. However, it is important to note that europium nitrate is a costly rare earth metal containing salt and strong oxidizer [6]. Hence, there is an urgent need to find alternative redox systems with properties of fast charge transfer and exhibiting photoelectrochemical behavior of CZTS absorber material. In this paper, we examine alternative electrolytes aiming to explore the enhanced photocurrent response in their respective applied potential range. We fabricate most of the CZTS thin films using electrodeposition-elevated temperature sulfurization on transparent conducting substrate. Some of the CZTS films are prepared using separately synthesized CZTS nanocrystals. The CZTS film qualities are finally evaluated for each

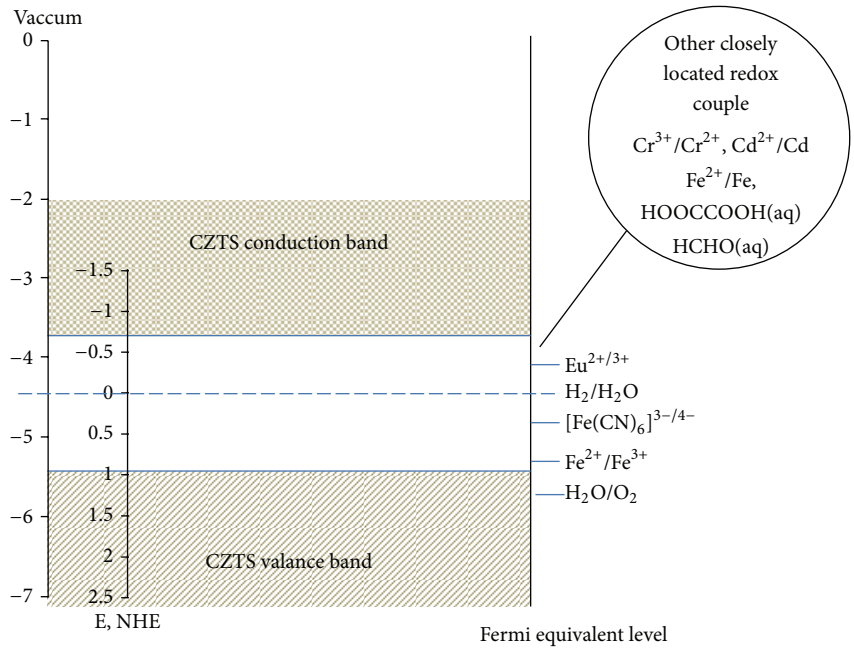

Figure 1: A schematic diagram showing CZTS band alignment with different redox electrolytes.

Table 1: Standard reduction potential for selected reactions.

No.	Electrode reaction	Standard reduction potential
1	$HCHO(aq) + 2H_2O + 2e^- \rightleftharpoons CH_3OH + 2OH^-$	−0.59 V
2	$2CO_2(g) + 2H^+ + 2e^- \rightleftharpoons HOOCCOOH(aq)$	−0.49 V
3	$Cr^{3+} + e^- \rightleftharpoons Cr^{2+}$	−0.42 V
4	$2SO_3^{2-} + 3H_2O + 4e^- \rightleftharpoons S_2O_3^{2-} + 6OH^-$	−0.58 V
5	$NO_2^- + H_2O + e^- \rightleftharpoons NO + 2OH^-$	−0.46 V

electrolyte system. It is important to mention that the fast developing area of plasmonics has great potential in enhancing the performance of the solar cells [7]. Plasmonics deals with the excitation of the surface plasmons which basically converts the light energy into electricity in the photovoltaic devices [8, 9]. Optical field enhancement in metallic nanostructures is generally utilized to achieve strong enhancement of optical absorption. Metallic nanoparticles or other dielectric nanocrystals support the energy collection of incident photons in surface plasmon oscillations. This energy can be subsequently transferred to the semiconductor substrate in a more efficient manner in comparison with the conventional photovoltaic CZTS absorber. These experiments and simulation are currently in progress. The present paper is organized as follow. In Section 2, we discuss the theory of the redox couple Cu_2ZnSnS_4 thin film band alignment. In Section 3, we discuss synthesis and characterization followed by results and discussion. The results are summarized in Section 5.

2. Theory

The important criterion for redox couple to be used for photoelectrochemical characterization of photovoltaic absorber layer is that, after reduction of one of the ionic species, it should not be deposited on the working electrode [3, 4]. Hence, many of the cost-effective redox couple cannot be used for this purpose due to electrodeposition. A schematic energy band alignment diagram (Figure 1) for CZTS has been drawn based on information from the literature [10, 11]. A Gaussian distribution of energy levels was assumed for oxidized and reduced species. It can be seen that conduction band offset for many redox species such as $Fe(CN)_6^{3-/4-}$, Fe^{2+}/Fe^{3+}, and H_2O/O_2 is very high. Hence, they will not be a good choice to record photoelectrochemical response. In the contrary, conduction band offset for Eu^{3+}/Eu^{2+} couple is relatively low. Moreover, that redox species is selected whose redox potential is in a range where no degradation of CZTS film occurs during electrochemical characterization [3, 4]. The standard electrode potential for Eu^{3+}/Eu^{2+} is ~−0.35 V (versus SHE) and it fulfills most of these requirements [3–5]. The schematic diagram shows only "estimated band position of CZTS" because exact values are not known due to ongoing research for this material. However, the species whose standard reduction potential is close to that of Eu^{3+}/Eu^{2+} can be well chosen. The standard electrode potential values for selected redox reactions are shown in Table 1 [12, 13]: the Fe^{2+}/Fe and Cd^{2+}/Cd also have standard reduction potential value close to Eu^{3+}/Eu^{2+}, with very small

band offset, but toxicity and deposition issue will create complications. $LiClO_4$ electrolyte in propylene carbonate was also utilized for photoelectrochemical study of CZTS films [14]. However, perchlorates form energetic mixtures in many organic compounds [15]. It is always recommended to choose redox electrolyte in which charge transfer process should be fast as well as reversible [16]. However, there are some reports where irreversible electrolytes were utilized as charge carrier scavenger [16]. In addition, CZTS is not only extensively used in solid photovoltaic cell but also it is being utilized as an electrochemical cell (EPC) [16, 17]. The "photosensitized electrolytic oxidation effect," a key phenomenon to understand solar water splitting, is now being utilized for CZTS material also. Hence, this paper will mainly focus on nonenergetic, cost-effective electrolytes.

3. Experimental

3.1. Material. Copper sulfate pentahydrate, zinc sulfate hexahydrate, tin chloride, chromium(III) chloride, sodium sulfite, formaldehyde, hydrated europium nitrate, potassium ferricyanide, potassium ferrocyanide, and oxalic acid were purchased from M/s. Sigma Aldrich. FTO coated glass substrate was purchased from M/s Pilkington USA.

3.2. Synthesis and Characterizations of CZTS Films. CZTS thin films were grown on fluorinated tin oxide coated glass substrate using solution-based methods. Two methods were utilized for CZTS thin film synthesis. In method 1, CZTS nanocrystals were produced separately and further coated on FTO substrate, whereas, for method 2, we utilized electrochemical techniques. For method 1, copper(II) acetate (99,999%), zinc(II) acetate (99,99%), tin(II) acetate anhydrous (≥97%), and thiourea (>99%) were grinded homogeneously. The molar composition was chosen in such a manner so that stoichiometric ratio of Cu : Zn : Sn in mixture was ~2 : 1 : 1. This mixture was sintered in the presence of evaporated sulfur environment for 2 hours at 550°C. The annealing tube (alumina) was purged with argon for 25 min to displace air, prior to sulfurization. Elemental sulfur (99.9%), placed on quartz boat, was held at a temperature of 150°C as the sulfur source. In another experiment, sintering was carried out without sulfur. After 2 hours, natural cooling was allowed and material was examined for phase detection. A sponge-type soft material was obtained, which easily turns into powder when grinded. This powder was washed in KCN (10% by weight solution in water) solution followed by washing in 50% aqueous solution of isopropyl alcohol to remove residual sulfide phases. CZTS powder was dissolved in isopropanol and stirred for 3 hours. For better adhesion, 3% cellulose was also mixed after stirring. Few drops of terpineol were also added in the solution. These nanocrystals were coated on FTO substrate by immobilizing using 1,2-ethanedithiol linkers. Nanocrystals coated film was further annealed (temperature ~300°C) in an argon environment for duration of 1 hour. For method 2, an electrolyte containing ions of interest (Cu^{2+}, Zn^{2+}, and Sn^{2+}) was used for growth of metallic layer [15, 18]. Coelectrodeposition was done by using 3-electrode cell connected to Gamry Instruments Reference 600 potentiostat operated by virtual front panel software. Electrodepositions were carried out at potential ~−1.6 V. Such films were annealed in evaporated sulfur environment to obtain CZTS thin film. A controlled sulfurization was carried out in a tube furnace to minimize film sheet resistance increment. Most of the sulfurized CZTS films were ~1 μm thick. An inert atmosphere was maintained using continuous supply of argon. CZTS films were characterized by X-ray diffraction, Raman, and inductively coupled plasma optical emission spectroscopy to verify phase and purity. More details about CZTS film synthesis, characterizations (such as morphology, roughness, and optical properties) and diode parameters of CZTS film on various back contact can be found in earlier reports [15, 18, 19].

Due to fact that XRD pattern of CZTS is very similar to that of other possible sulfides, phase examination was carried out using Raman spectroscopy. An R 3000 QE Raman spectrometer (made by Raman Systems) was used for Raman spectroscopy. A laser excitation of wavelength ~ 785 nm was used for Raman measurements. The laser power was ~100 mW. Scanning electron microscopy was performed using an FEI Quanta 600TM scanning electron microscope. Band gap measurements of CZTS thin films were done using transmittance data obtained from an Ocean Optics spectrophotometer equipped with OOI Base 32 software [15, 18]. *J-V* curves were recorded during LED light illumination (incident illuminance on substrate ~3.2×10^4 lux at wavelength of ~550 nm)) and in dark by using a Gamry Instruments Reference 600 potentiostat regulated by virtual front panel software. An equivalent concentration of all electrolytes solutions was ~0.07 mole/l. In a typical experiment a CZTS coated thin film on FTO substrate was immersed in an aqueous solution of redox electrolyte together with a saturated calomel reference electrode (SCE) and a platinum counter electrode for measurements. The details of photoelectrochemical characterization experiments can be found in earlier report [3]. 3D topographical images were captured by using an AmScope eyepiece camera equipped with ToupView 3.2 software.

A flat band potential measurement was also carried out in order to estimate contribution from space charge current. Three-electrode electrochemical cell was used for flat band measurements. Mott-Schottky analysis was carried out for flat band potential evaluation. A substrate containing CZTS thin film grown on FTO coated glass was immersed in various electrolytes. The following equation was used for flat band potential calculation [3]:

$$\frac{1}{C_{sc}^2} = \frac{2}{e\varepsilon_s\varepsilon_0 N}\left[\left(V - V_{fb}\right) - \frac{K_B T}{e}\right], \quad (1)$$

where C_{sc} is capacitance of the depletion region and K_B is Boltzmann's constant. The flat band potential was evaluated by extrapolation to $1/C^2 = 0$ in the Mott-Schottky plot. "N" is the doping density, "e" represents electronic charge, "V" is applied potential, and "T" represents temperature. ε_s is the dielectric constant of the semiconductor; ε_0 is the permittivity of free space.

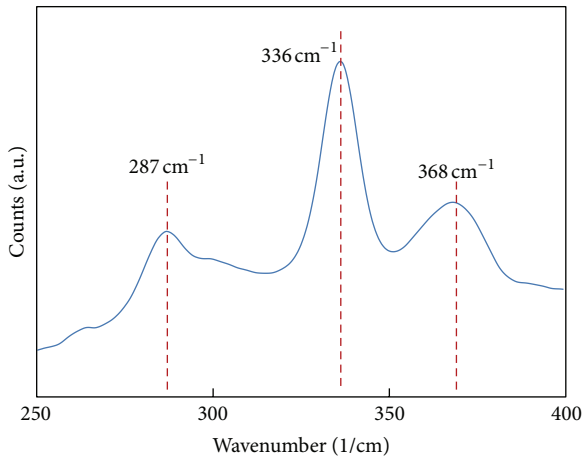

Figure 2: Raman spectrum of CZTS nanopowder.

4. Results and Discussion

Figure 2 shows the Raman spectrum of the CZTS powder over the range from 200 to 400 cm^{-1}. In the Raman spectrum an obvious major peak located at 336 cm^{-1} and two minor peaks at 368 cm^{-1} and 287 cm^{-1} can clearly be seen. This spectral data is in good agreement with the reported Raman spectra of CZTS [5]. SEM images of CZTS powder (on conducting substrate) and film surface are also shown in Figure 3. It can be seen that nanoparticles size is variable (Figure 3(a)). Few of them are less than 50 nm, while some of the particles are greater than 100 nm. Grains of CZTS film are ~1 μm big, although we obtained some small-size particles (see Figure 3(b)).

The formation of conformal contact between CZTS and europium nitrate electrolyte promotes the minimization of minority carrier diffusion towards electrolyte [4]. For redox couples enlisted in Table 1, a similar phenomenon can be expected. Detailed discussion about photocurrent generation phenomenon during illumination can be found in earlier reports [3, 4]. For evaluation of photoelectrochemical performance, linear scan voltammograms were recorded by the potentiostat using virtual front panel software during flashing light illumination. The cathodic photocurrent response confirms p-type photoactivity of the annealed CZTS films. We examined both of our films (from nanocrystal suspension and electrochemically grown) for photoelectrochemical test, and we found that photocurrent for film grown by electrodeposition-sulfur annealing is relatively high. Small photocurrent response for nanocrystalline film can be attributed to high recombination and short lifetime of carrier. Hence, we conducted most of our experiments using film grown by method 2. We have evaluated change in current during illumination at different potential for different redox couples and average change in current during illumination is plotted in the same graph for comparison (see Figure 4). It can be seen that, for Cr^{3+}/Cr^{2+} redox couple, change in photocurrent (ΔI) is maximum for small potential range (0 V to −0.5 V). However, we were not able to characterize our film beyond this potential range due to its degradation. On the other hand, all other proposed electrolytes showed photocurrent response up to potential 0.8 V. Specifically, both Eu^{3+}/Eu^{2+} redox couple and oxalic acid show significant change in photocurrent up to a potential of ~1 volt. But it is interesting to note that maximum change in photocurrent using oxalic acid as an electrolyte was twice as high compare, to europium nitrate electrolyte solution. Formaldehyde, sulfite, and nitrite couples also showed photoelectrochemical response, but change in photocurrent is approximately half compared to that with europium nitrate. It is essential to understand that enhanced cathodic photocurrent during illumination indicates an occurrence of reduction reaction. For oxalic acid case, it is possible due to presence of CO_2 along with H^+ in water. Although effects and actual content of dissolved CO_2 in context of CZTS are not well studied, some reports discussed aspects of dissolved CO_2 for other kind of wafers [20]. For this study, we have neglected dissolved CO_2 contribution. Hence, it is very likely that cathodic photocurrent generation in this case is due to reduction of H^+ into hydrogen gas. A separate comparative test was conducted using solution of sulfuric acid and oxalic acid with similar pH. It can be seen that photocurrent (Figure 5) is still high compare to that from sulfuric acid case. It illustrates that there are other additional operative mechanisms in case of oxalic acid aqueous solution which causes enhanced photovoltaic performance. This observation is encouraging and can be utilized as selective conversion of CO_2 to oxalate in water.

In order to confirm whether alternative electrolytes can cause any phase change or degradation in CZTS absorber deposited on FTO, Raman spectroscopy was carried out. Figure 6 shows Raman spectra of a film (before and after electrochemical test) over the range from 250 to 400 cm^{-1}. In all Raman spectra the two peaks are located at 336.5 and 367.5 cm^{-1} and it can be clearly seen that peak at ~336.5 cm^{-1} is stronger peak. The Raman peak positions and relative intensities are in good agreement with the previously reported Raman spectra of CZTS thin film [5, 15]. No significant change in Raman spectra of film was observed after electrochemical test in sodium sulfite, formaldehyde, or sodium nitrite solution. After Lorentzian function fitting to both spectra, it was observed that both Raman linewidth and peak intensity did not change significantly which indicates that CZTS film's phase integrity is not disrupted after photoelectrochemical examination in oxalic acid aqueous solution.

A comparison of film surface topography is shown in Figure 7. To evaluate larger film area, we used lower magnification images for analysis. A change in surface topography can be seen when the film is exposed to europium nitrate electrolyte solution. In an encircled area, one can observe some changes in film roughness. Thorough analysis suggests that less than ~20% of film area was changed. However, there was more change in surface features and topography (>45% of film area) when electrochemical tests were run using oxalic acid electrolyte solution. For Cr^{3+}/Cr^{2+} redox couple, we observed huge change in surface topography (see Figure 8). Such films were not suitable for topography comparison after an electrochemical test. However, an optical image showing damaged portion of film is shown for comparison. Almost

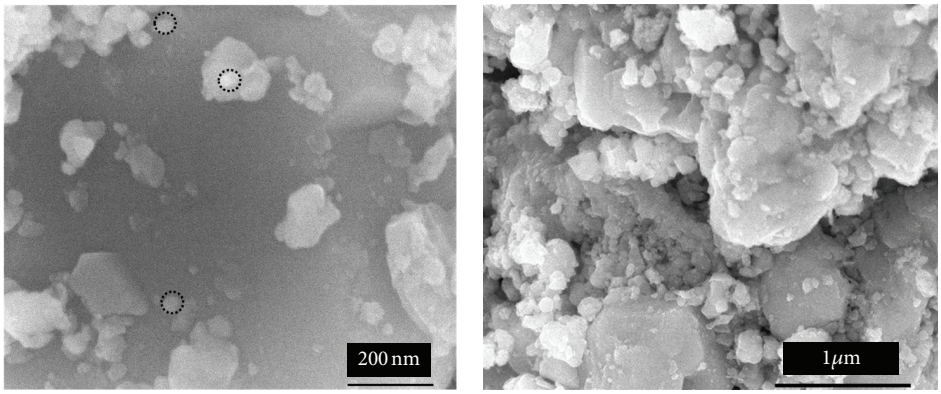

(a) (b)

FIGURE 3: Scanning electron micrograph of (a) CZTS nanocrystals on copper substrate (nanoparticles of size ~50 nm are shown within circle); (b) CZTS thin film, grown using nanocrystals.

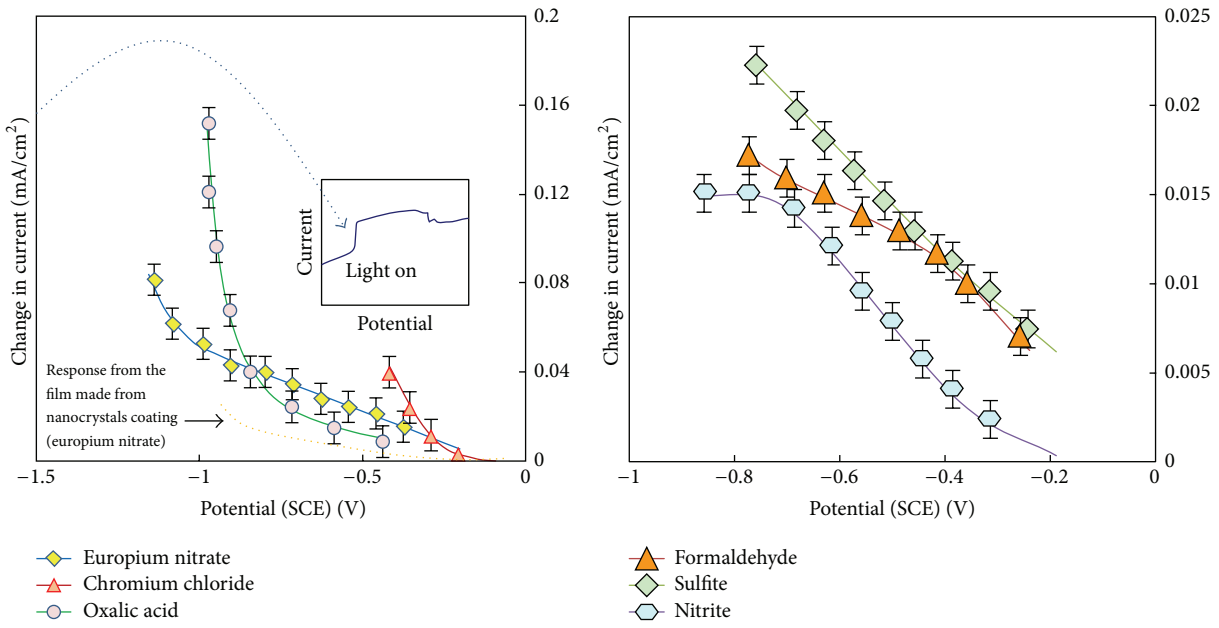

(a) (b)

FIGURE 4: Average photoelectrochemical response of CZTS thin film in different redox electrolytes, change in current during illumination is shown in inset.

no change in film topography was observed when photoelectrochemical tests were run using formaldehyde, sodium sulfite, and sodium nitrite solutions. An estimation of ionic species concentration, pH, and ionic strength was carried out using Visual MINTEQ software, in order to evaluate effects of these parameters. It was observed that oxalic acid, a strong acid, has lower pH value compared to that of europium nitrate aqueous solution. Hence, we can expect more change in surface topography in case of oxalic acid. Chromium chloride solution is also slightly acidic but acidity is less compare, to oxalic acid solution. For sulfite and nitrite photoelectrochemical reaction causes creation of OH^- ion, still we did not observe any significant change in surface topography. A photocatalytic oxidation of SO_3^{2-} into $S_2O_6^{2-}$ is reported [18], along with good amount of hydrogen production in the presence of mercury lamp. The kinetics of reported reaction is a multistage photolytic process and depends on several factors such as pH, concentration, temperature, and reaction pathways [21]. It is very likely that such mechanisms are operative; hence, we conducted a control test using a different copper working electrode. We did not observe any reportable change in photoactivity in this case. Hence, it can be said that most of the photoactivity is due to reduction of sulfite ion via CZTS-electrolyte charge transfer mechanism.

It can be seen that electrode reactions 1 and 4 (sulfite and formaldehyde) have shown higher photoelectrochemical response, whereas reaction 5 (nitrite) has relatively low photocurrent. Nitrite has good absorptivity in water; a broad

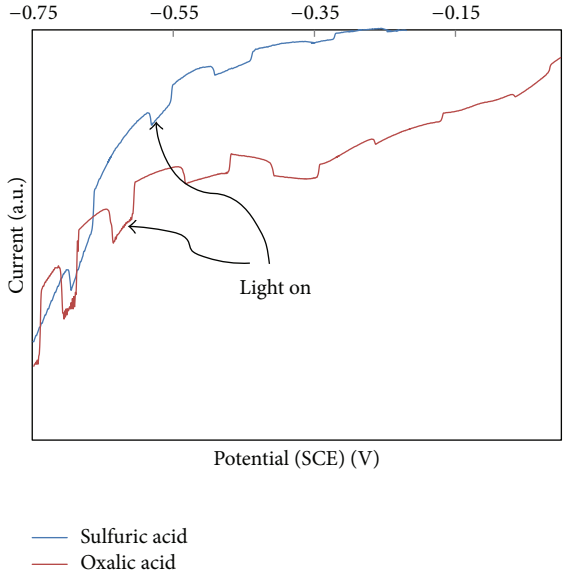

Figure 5: A comparison of current potential behavior/photoelectrochemical response of CZTS thin film in oxalic acid and sulfuric acid solution.

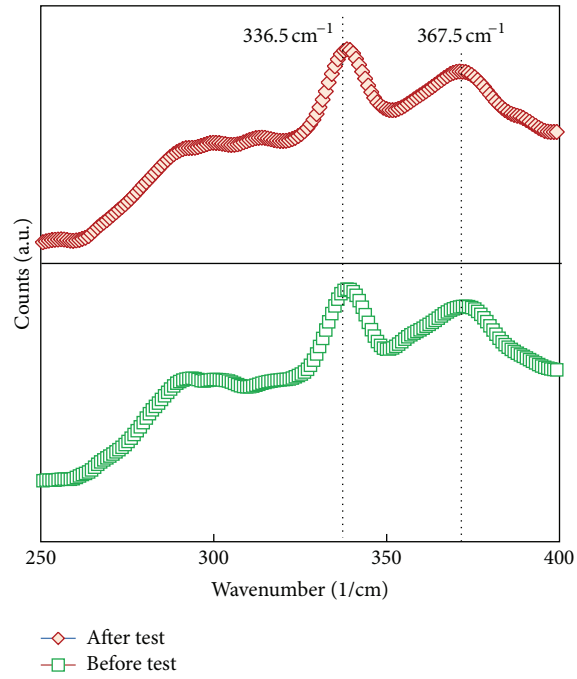

Figure 6: (a) Raman spectra of CZTS film before and after test in europium nitrate solution (b) Raman spectra of CZTS film before and after test in oxalic acid aqueous solution. No significant change in Raman spectra was found after electrochemical test in formaldehyde, sodium sulfite, or sodium nitrite solution.

peak, centered at 355 nm corresponds to $n \rightarrow \pi^*$ transition [22]. At shorter wavelength it shows absorption due to $\pi \rightarrow \pi^*$ transition. Specifically for nitrite, photolysis process and species consumption/production involve a number of reactions; hence, it is difficult to measure individual rate of reaction. However, strong absorptivity in water can cause effective reduction of photons incident to CZTS film. We carried out a similar control test, what we conducted for sodium sulfite, and did not find any measurable contribution to total photoelectrochemical current. Despite the low photocurrent, it can be advantageous to use sodium nitrite because of its good corrosion inhibition properties [23].

The situation when defect states locate within center of the band gap can cause exchange of charge either from valence band or conduction band. There is a possibility that valance bandmediated charge transfer mechanism is operative and contributing to effective photoelectrochemical response. A separate experiment was conducted to investigate this phenomenon, where photoelectrochemical response of CZTS thin film was measured using Fe $(CN)_6^{3-/4-}$ redox couple. From Figure 1, it can be seen that $Fe(CN)_6^{3-/4-}$ redox couple is good choice, because its equivalent Fermi level lies very close to mid gap. Figure 9 shows the current potential behavior of CZTS working electrode immersed in $Fe(CN)_6^{3-/4-}$ during illumination and dark. It can be seen that there is not any good photocurrent response, indicating that most of the photoelectrochemical response in case of CZTS is due to conduction band-mediated charge transfer mechanism.

The total current is an aggregate of dark current, photocurrent, and space charge recombination current [3]. The photocurrent is a direct function of number of free electron in field free region (n). The value of "n" depends on many factors such as recombination rate, heterogeneous charge transfer rate, diffusion rate of electron, and intensity loss of photons during travel inside the solution. For similar substrate, incident power, and absorption coefficient of film, photocurrent contribution from each electrolyte was assumed to be same (light absorption in electrolyte was also assumed to be similar except for Cr^{3+}/Cr^{2+}). Contribution from space charge current (J_{SCR}) depends mainly on relative difference between flat band potential and applied voltage [3]:

$$J_{SCR} = B\sqrt{\left|\left(V_{fb} - V\right)\right|}e^{qV/2K_BT}, \quad (2)$$

where "B" is a recombination constant. The value of "B" depends on various factors including carrier thermal velocity, density of traps, and capture cross-section. For a similar value of "B," the flat band potential will govern the change in J_{SCR}. It was observed that flat band potential for oxalic acid electrolyte is ~120 mV more than europium redox couple (see Figure 10). The lowest flat band potential was observed for sodium sulfite electrolyte. Altogether, it can be said that the square root term in (2) and subsequent space charge current will be different for these electrolytes. It was observed that such contribution or change is more effective towards anodic direction; however, most of our photoelectrochemical characterization was done at negative potential.

For large negative electrode potential, cathodic reaction at CZTS will be mainly due to transport control, and there will be significant loss of interfacial charge transfer control

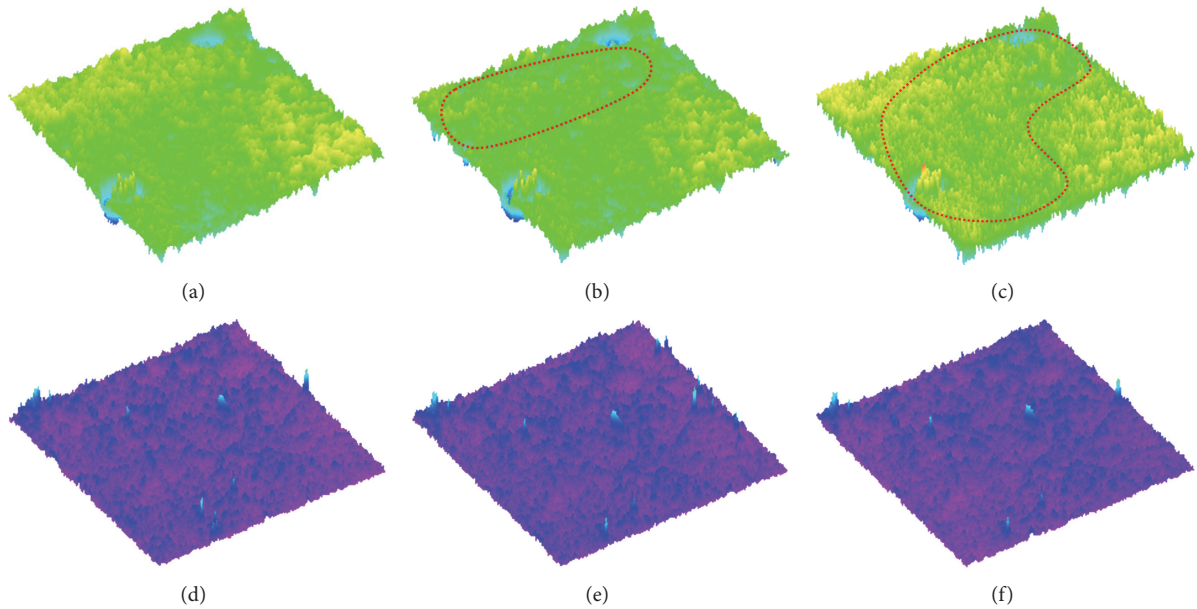

FIGURE 7: 3D topography of CZTS film (area ~50 $\mu\times$ 50 μ). (a) Before electrochemical test in europium nitrate aqueous solution, (b) After electrochemical test in europium nitrate solution. (c) After electrochemical test in oxalic acid aqueous solution. (d) Before electrochemical test in formaldehyde aqueous solution. (e) After electrochemical test in formaldehyde aqueous solution. (f) After electrochemical test in sodium sulfite aqueous solution.

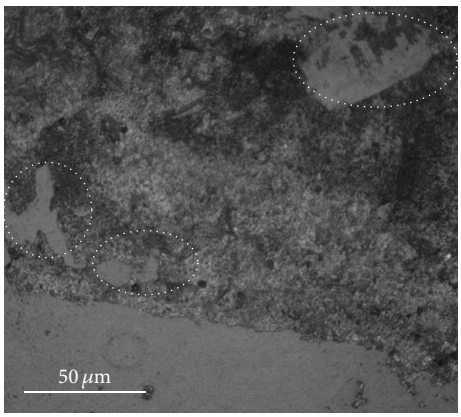

FIGURE 8: An optical micrograph of CZTS film after electrochemical test in chromium chloride solution; damaged film can be seen within encircled area.

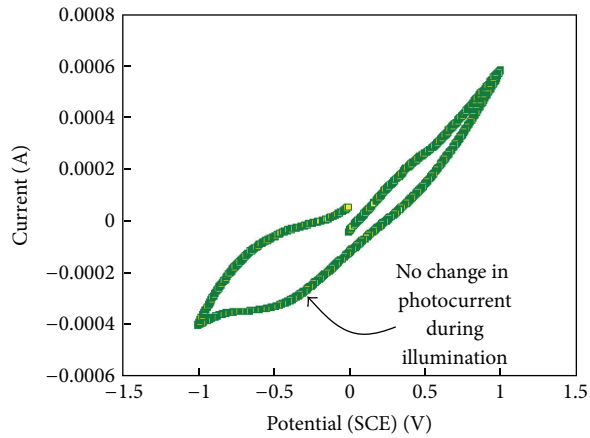

FIGURE 9: Current potential behavior of CZTS thin film grown on FTO coated glass and immersed in redox electrolytes containing $Fe(CN)_6^{3-/4-}$ redox couple, during flashing light illumination.

[24]. The adsorbed "intermediate radicals" are also very important to explain photoelectrochemical kinetics [24]. In our case, these radicals are different because of different electrolytes (and their solution parameters), and hence there is possibility of different surface states. The charge transfer rate constant is related to drift velocity of outgoing electron and density of acceptor states, which can be different for different electrolytes [3, 24]. It is believed that acidity of oxalic acid causes production of dangling bond. Density of such defect states changes exponentially due to change in potential [18]. For most of the redox reaction, the contribution of surface states was assumed to be minimal, and rate (current) determining step is due to Schottky barrier type transport.

Although majority of change in dark current beyond the standard reduction potential is due to reduction of one of the ionic species in solution [4], adsorption of species in electrode also causes change in rate kinetics [23]. It should be noted that most of the adsorbed species are different. The surface recombination rate constant is an important and highly sensitive parameter and it causes significant change in photocurrent when its value is changed twice of the original value [3]. Hence, it will be interesting to explore the effects of all these parameters as well as plasmonic effects [25] in detail; these experiments are in progress.

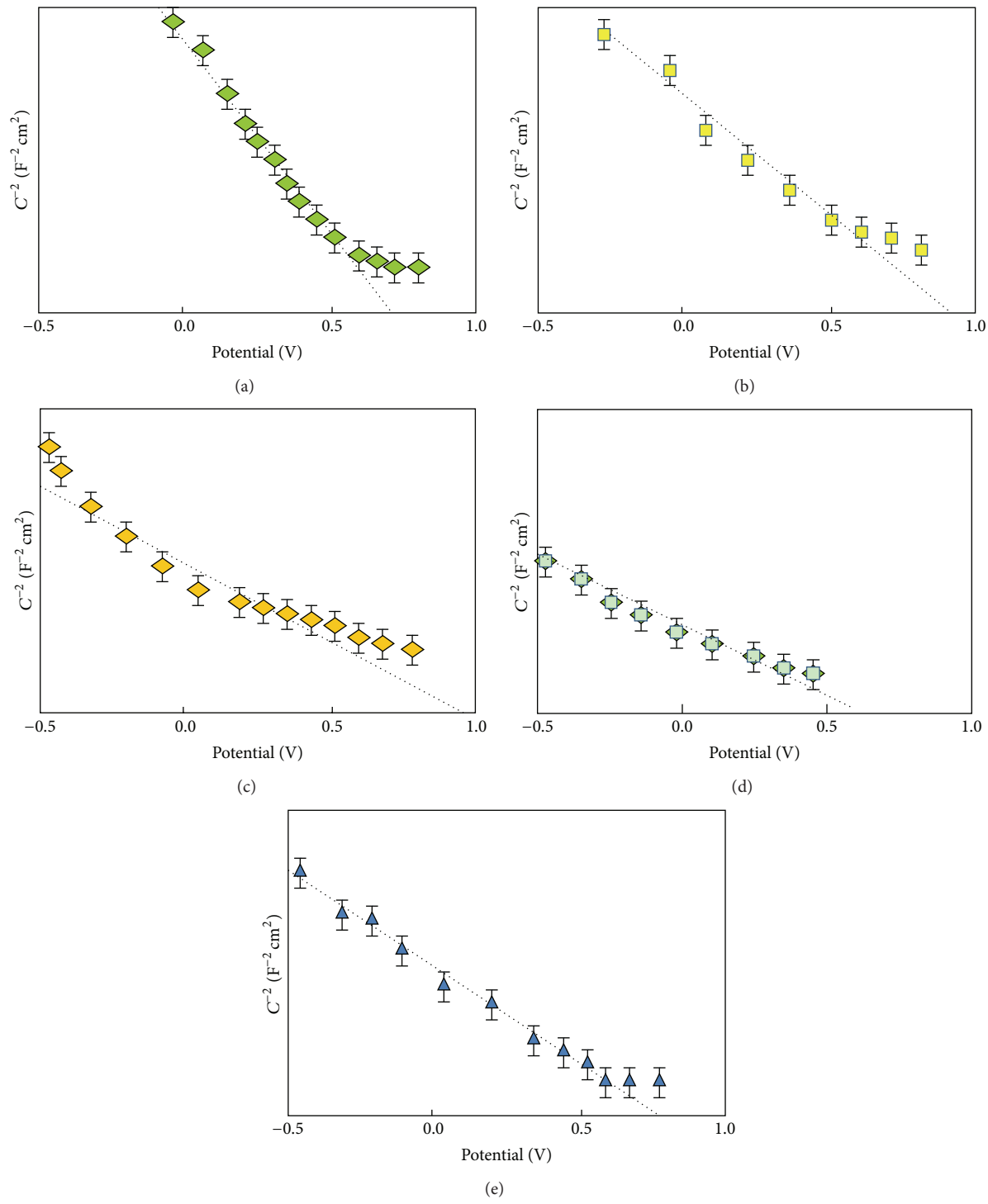

Figure 10: (a) Mott-Schottky plot for CZTS film grown on FTO coated glass substrate and (a) immersed in europium nitrate solution, (b) immersed in oxalic acid aqueous solution, (c) immersed in sodium nitrite aqueous solution, (d) immersed in sodium sulfite aqueous solution, and (e) immersed in formaldehyde aqueous solution.

5. Conclusions

In summary, alternative electrolytes were examined to evaluate photoelectrochemical performance of CZTS absorber materials. Our primary results suggest that these electrolytes/redox couples can be beneficial due to equivalent or enhanced photocurrent response in their respective applied potential range. However, more details such as irreversibility and charge transfer process for these electrolytes are still needed to explore. In case of sodium sulfite and formaldehyde, photoelectrochemical response was satisfactory, whereas for sodium nitrite photocurrent was less. It was

observed that oxalic acid aqueous solution acts very well over the potential range of ~−0.5 V to −1.0 V. Film quality and topography were evaluated by comparing 3D topographical image and it was observed that oxalic acid redox couples cause less damage in surface features while for Cr^{3+}/Cr^{2+} redox couple film damage was high. Almost no damage was observed in CZTS thin film when sodium sulfite, formaldehyde, and sodium nitrite were used as redox scavenger. A difference in photocurrent for different electrolytes was explained on the basis of different defect states, adsorption of species in photoelectrode, and different surface recombination rate constant.

References

[1] T. K. Todorov, K. B. Reuter, and D. B. Mitzi, "High-efficiency solar cell with earth-abundant liquid-processed absorber," *Advanced Materials*, vol. 22, no. 20, pp. E156–E159.

[2] T. K. Todorov, J. Tang, S. Bag et al., "Beyond 11% efficiency: characteristics of state-of-the-art $Cu_2ZnSn(S,Se)_4$ solar cells," *Advanced Energy Materials*, vol. 3, no. 1, pp. 34–38, 2012.

[3] P. K. Sarswat and M. L. Free, "An evaluation of depletion layer photoactivity in Cu_2ZnSnS_4 thin film," *Thin Solid Films*, vol. 520, no. 13, pp. 4422–4426, 2012.

[4] S. C. Riha, S. J. Fredrick, J. B. Sambur, Y. Liu, A. L. Prieto, and B. A. Parkinson, "Photoelectrochemical characterization of nanocrystalline thin-film Cu_2ZnSnS_4 photocathodes," *ACS Applied Materials and Interfaces*, vol. 3, no. 1, pp. 58–66, 2011.

[5] P. K. Sarswat and M. L. Free, "Demonstration of a sol-gel synthesized bifacial CZTS photoelectrochemical cell," *Physica Status Solidi (A)*, vol. 208, no. 12, pp. 2861–2864, 2011.

[6] http://www.sigmaaldrich.com.

[7] V. E. Ferry, M. A. Verschuuren, H. B. T. Li et al., "Light trapping in ultrathin plasmonic solar cells," *Optics Express*, vol. 18, no. 13, pp. A237–A245, 2010.

[8] C. S. Liu, G. Kumar, and V. K. Tripathi, "Laser mode conversion into a surface plasma wave in a metal coated optical fiber," *Journal of Applied Physics*, vol. 100, no. 1, Article ID 013304, 6 pages, 2006.

[9] G. Kumar and V. K. Tripathi, "Excitation of a surface plasma wave over a plasma cylinder by a relativistic electron beam," *Physics of Plasmas*, vol. 15, no. 7, Article ID 073504, 5 pages, 2008.

[10] S. Chen, J. H. Yang, X. G. Gong, A. Walsh, and S. H. Wei, "Intrinsic point defects and complexes in the quaternary kesterite semiconductor Cu_2ZnSnS_4," *Physical Review B*, vol. 81, no. 24, Article ID 245204, 10 pages, 2010.

[11] M. Grätzel, "Photoelectrochemical cells," *Nature*, vol. 414, pp. 338–344, 2001.

[12] http://www.ed.gov.nl.ca/edu/k12/evaluation/chem3202/standardreductionpotentials.pdf.

[13] N. A. Lange, *Lange Handbook of Chemistry*, Mcgraw-Hill, New York, NY, USA, 9th edition, 1956.

[14] N. M. Shinde, D. P. Dubal, D. S. Dhawale, C. D. Lokhande, J. H. Kim, and J. H. Moon, "Room temperature novel chemical synthesis of Cu_2ZnSnS_4 (CZTS) absorbing layer for photovoltaic application," *Materials Research Bulletin*, vol. 47, no. 2, pp. 302–307, 2012.

[15] H. Vogt, J. Balej, J. E. Bennett, P. Wintzer, S. A. Sheikh, and P. Gallone, "Chlorine oxides and chlorine oxygen acids," in *Ullmann'S Encyclopedia of InduStrial ChemiStry*, John Wiley & Sons, New York, NY, USA, 2000.

[16] P. K. Sarswat and M. L. Free, "A Comparative study of Co-electrodeposited Cu_2ZnSnS_4 absorber material on fuorinated tin oxide and molybdenum substrates," *Journal of Electronic Materials*, vol. 41, no. 8, pp. 2210–2215, 2012.

[17] R. C. Alkire, D. M. Kolb, J. Lipkowski, and P. N. Ross, *Photoelectrochemical Materials and Energy Conversion Process*, Wiley-VCH & Co. KGaA, Weinheim, Germany, 2010.

[18] H. Cherfouh, T. Chari, A. Guermoune, M. Siaj, and B. Marsan, "Preparation and characterization of a new $CuInS_2$/Graphene composite electrode, for application in electrochemical solar cells," in *Proceedings of the 219th Electrochemical Society (ECS) Meeting*, abstract 1870, 2011.

[19] P. K. Sarswat, M. L. Free, and A. Tiwari, "A factorial design of experiments approach to synthesize CZTS absorber material from aqueous media," in *Novel Fabrication Methods for Electronic Devices*, L. Schmidt-Mende, H. J. Snaith, G. L. Whiting, and D. S. Ginger, Eds., abstract G6.18, 2010, Proceedings of the Materials Research Society Symposium, Boston, Mass, USA, vol. 1288, 2011.

[20] P. K. Sarswat and M. L. Free, "an assessment of contact engineering for the Cu_2ZnSnS_4-alternative back contact," *Materials Focus*, vol. 2, no. 4, pp. 244–250, 2013.

[21] S. Kumari, M. Keswani, S. Singh et al., "Effect of dissolved CO_2 in de-ionized water in reducing wafer damage during megasonic cleaning in megpie," *ECS Transactions*, vol. 41, no. 5, pp. 93–99, 2011.

[22] C. Huang, C. A. Linkous, O. Adebiyi, and A. T-Raissi, "Hydrogen production via photolytic oxidation of aqueous sodium sulfite solutions," *Environmental Science and Technology*, vol. 44, no. 13, pp. 5283–5288, 2010.

[23] M. Fischer and P. Warneck, "Photodecomposition of nitrite and undissociated nitrous acid in aqueous solution," *Journal of Physical Chemistry*, vol. 100, no. 48, pp. 18749–18756, 1996.

[24] S. I. Krakhmalev, V. A. Vorotnikova, N. V. Ten, and N. V. Taranova, "Determination of sodium nitrite in complex sodium grease," *Chemistry and Technology of Fuels and Oils*, vol. 20, no. 12, pp. 612–613, 1984.

[25] Y. K. Mishra, R. Adelung, G. Kumar et al., "Formation of self-organized silver nanocup type structures and their plasmonic absorption," *Plasmonics*, vol. 8, pp. 811–815, 2013.